Online ISSN: 2981-0396 Print ISSN: 2981-0388

International Journal of Iron & Steel Society of Iran

Journal Homepage: https://journal.issiran.com/

Research Article

Effect of Intercritical Annealing Temperature and Time on Microstructure and Tensile Properties of a Step-Quenched Dual Phase Steel

H. Ashrafi *[1], Z. Soleimani Bistegani [2]

Faculty of Chemical and Materials Engineering, Shahrood University of Technology, Shahrood, Iran

ARTICLE INFO

Keywords:

Dual phase steel, Step-quenching, Intercritical annealing, Microstructure, Tensile properties.

Article history:

Received 08 February 2025
Received in revised form 03 May 2025
Accepted 05 August 2025

ABSTRACT

A heat treatment cycle involving step-quenching followed by intercritical annealing (IA) at 740°C, 770°C and 800°C for times between 2-12 min was utilized to produce dual-phase (DP) steels. The microstructural analysis revealed that the martensite islands formed during step-quenching were refined significantly after IA. The final DP steels contained ferrite grains of two sizes distribution: coarse grains ranging from 10 to 25 µm and ultrafine grains smaller than 2 µm. The martensite islands displayed two morphologies: fine and fibrous martensite in samples annealed at 740°C and 770°C and equiaxed martensite islands in all samples. Continuous yielding behavior was observed in all samples except those annealed at 740°C for 2- and 4-min. IA at all temperatures led to a decrease in yield stress and ultimate tensile strength, with enhancements in uniform elongation and total elongation only observed after IA at 740°C and 770°C. The sample annealed at 770°C for 12 min exhibited the best combination of tensile properties for auto body applications. The samples displayed a three-stage work-hardening behavior based on the modified Crussard–Jaoul analysis, however the third stage was absent in samples annealed at 740°C for 7 and 12 min due to the high carbon content of the martensite.

1. Introduction

Dual-phase (DP) steels, a prominent group of the advanced high-strength steels (AHSS) family, are commonly used in various auto body structures such as bumper reinforcement, A-pillars, door beams, and frame parts [1, 2]. Their unique microstructure, featuring 10-50 vol.% hard martensite islands surrounded by a ductile ferrite matrix, grants them exceptional mechanical properties, including continuous yielding behavior, a low yield stress (YS) to ultimate tensile strength (UTS) ratio, high initial work-hardening rate, and good formability. These desirable attributes, along with their straightforward chemistry, good weldability, and cost-effectiveness, have made DP steels a preferred choice for the automotive industry [3-7].

Despite their wide application in the auto industry, DP steels cannot compete with the newer grades of the AHSS in terms of strength and ductility. The strength-elongation balance of quench and partitioned steels can exceed 37000 MPa% [8], while that of DP steels barely goes over 20000 MPa% [9]. This prompted researchers to focus on improving the mechanical properties of DP steels through

* *Corresponding Author*
Email: hashrafi@shahroodut.ac.ir
Address: Faculty of Chemical and Materials Engineering, Shahrood University of Technology, Shahrood, Iran
1. Assistant Professor, 2. B.Sc.

DOI: http://10.22034/IJISSI.2025.2052973.1318
Published by ISSI (Iron & Steel Society of Iran)

methods such as the addition of alloying elements [10], thermomechanical processing [11, 12] and introduction of second-phase dispersoids [13]. Some researchers have also explored the use of double-step or repetitive intercritical annealing (IA) to enhance the mechanical properties of DP steels. In the first study, Ashrafi et al. [14] used a double-step IA to produce a DP steel with chain-like networked martensite islands within the ferrite matrix. They observed an improvement of above 50% in the elongation compared to the conventional IA without sacrifying the UTS. In another study, Ghaemifar and Mirzadeh [15] performed a three-step IA on low-carbon steel with a fully martensitic microstructure. They found that this repetitive IA was effective in enhancing the strength-elongation balance. They also reported a two-fold increase in tensile strength compared to the single-step IA at the same level of ductility. Khebreh Farshchi et al. [16] also found repetitive IA helpful in enhancing the mechanical properties and work-hardening behavior of DP steels. Saenarjhan et al. [17] used a double-step IA to modify the mechanical properties of DP steel. Their results showed that double-step IA increases ductility without losing a significant amount of strength. Ding et al. [18] used repetitive IA to produce a DP steel with a lamellar ferrite-martensite microstructure. They reported a significant improvement in ductility while the UTS dropped marginally.

The above reviewed literature suggested that the repetitive IA could enhance the mechanical properties of DP steels. However, these studies only focused on using either ferrite-martensite or fully martensitic initial microstructures. In this study, a new method incorporating step-quenching and IA heat treatment cycles was developed to produce DP steels. The impact of IA temperature and time on the microstructure, tensile properties, and work-hardening behavior was also investigated in this research.

2. Materials and Methods

The material used in this research was a low carbon steel with the chemical composition listed in Table 1. The steel was provided in the form of a cold-rolled sheet with the thickness of 2 mm.

The initial steel underwent a step-quenching heat treatment cycle, according to Fig. 1. and then annealed at various intercritical temperatures for 2, 4, 7 and 12 min, followed by water quenching (WQ). The critical temperatures of A1 and A3 were determined by following equations [19]:

$$A_1 = 723 - 10.7\,Mn + 29.1Si - 16.9\,Ni + 16.9Cr + 290\,As + 6.38W \quad \text{Eq.(1)}$$

$$A_3 = 910 - 203\sqrt{C} + 44.7\,Si - 15.2\,Ni + 104V + 31.5\,Mo + 13.1W \quad \text{Eq.(2)}$$

The microstructure of the cross-section of samples was examined by optical microscopy (OM) in a DeWinter DEW/150 microscope, and scanning electron microscopy (SEM) in a Zeiss sigma300-HV field emission SEM. Specimens for the microstructural analysis were mounted, grounded to a 2500 grit finish, polished with a 0.3 µm alumina suspension, and etched in a 2% Nital solution. The grain size of ferrite in the DP steels was determined by the mean intercept method according to the ASTM E112-13 standard [20]. The volume fraction of martensite (V_M) in the DP steels was evaluated by the point counting method according to the ASTM E562-19 standard [21]. The Image J software was utilized to assess both the grain size and the volume fraction of phases.

Tensile specimens (6.4 mm gauge length, 25 mm length, 6 mm width) were cut from the heat-treated steels perpendicular to the initial rolling direction by electrical discharge machining (EDM). The specimens were then tested in a SANTAM STM150 machine at a constant cross-head speed of 1 mm/min at room temperature. Three specimens were tested for each condition to obtain an average value for the tensile properties.

3. Results and Discussion

3.1. Microstructural Observations

Fig. 2a. displays the initial steel's microstructure, which includes elongated ferrite grains (bright) and pearlite colonies (dark) in the rolling direction (RD). The microstructure of the step-quenched sample (Fig. 2b.) consisted of ~50 vol.% large and blocky martensite islands (dark) within the ferrite matrix (bright). The size of the martensite islands ranged from 5 to 25 µm, with a few islands having larger diameters. The average grain size of ferrite was measured at 8.9 ± 0.7. This type of microstructure, characterized by large martensite islands within a coarse-grained ferrite matrix, is commonly observed in step-quenched DP steels[22, 23].

Table 1. Chemical composition (wt.%) of the initial steel.

C	Mn	Si	S	P	Ni	Mo	Cu	V	Al	Co	Nb	Zr	Fe
0.18	1.25	0.2	0.01	0.011	0.015	0.019	0.019	0.02	0.073	0.045	0.023	0.011	Bal.

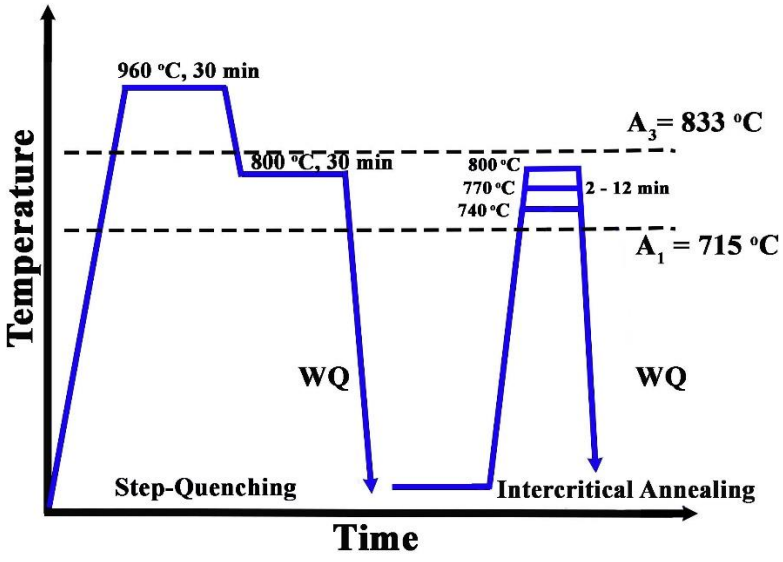

Fig. 1. Schematic of the heat-treatment cycles used in this study.

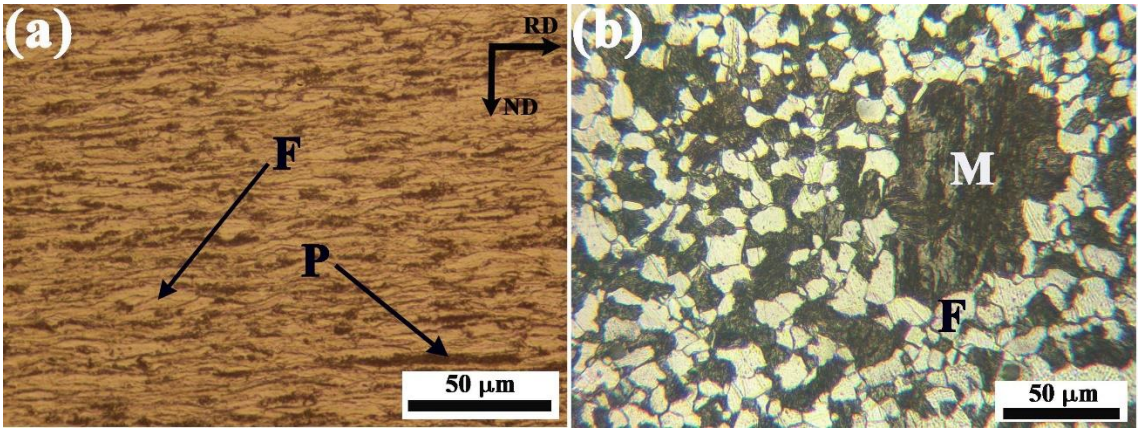

Fig. 2. OM microstructure of (a) initial steel, and (b) step-quenched steel. F: ferrite, P: pearlite, M: martensite.

The representative microstructure of the step-quenched sample after IA at different temperatures for various durations is illustrated in Fig. 3. It was evident that the martensite islands were significantly refined after IA. However, the size of the martensite islands varied depending on the annealing temperature, with larger sizes seen at higher temperatures. The distribution of martensite islands within the ferrite matrix was also non-uniform. Two different morphologies of martensite islands were identified: equiaxed martensite islands present in all samples, and fine and fibrous martensite mainly found in samples annealed at 740°C and 770°C. The ferrite grains exhibited two sizes distributions: coarse grains between 10 and 25 µm inherited from the initial step-quenched sample, and ultrafine grains smaller than 2 µm formed during IA. These ultrafine grains were surrounded by martensite islands. Previous studies have shown that annealing a martensitic microstructure leads to the formation of fine and fibrous martensite in the ferrite matrix [24]. The high density of boundaries between martensite laths provides numerous nucleation sites for austenite phase at intercritical temperatures, dividing the martensite block into ultrafine ferrite grains and martensite islands. As most of the austenite pools at intercritical temperature form within existing martensite blocks, a non-uniform distribution of martensite islands persists after annealing.

Fig. 4. shows the relationship between martensite volume fraction (V_M) and average ferrite grain size (D_F) with the annealing time at different temperatures. V_M was found to be primarily influenced by the IA temperature, rather than by annealing time. This is in contrast to previous works, which stated that V_M is changed with IA time [25]. D_F was found to be affected by both annealing temperature and time, with D_F decreasing as the annealing temperature increased and the annealing time decreased. The decrease in D_F at higher annealing temperatures was attributed to the increase in V_M. Previous studies have also shown a linear reduction in D_F with increasing V_M.[19].

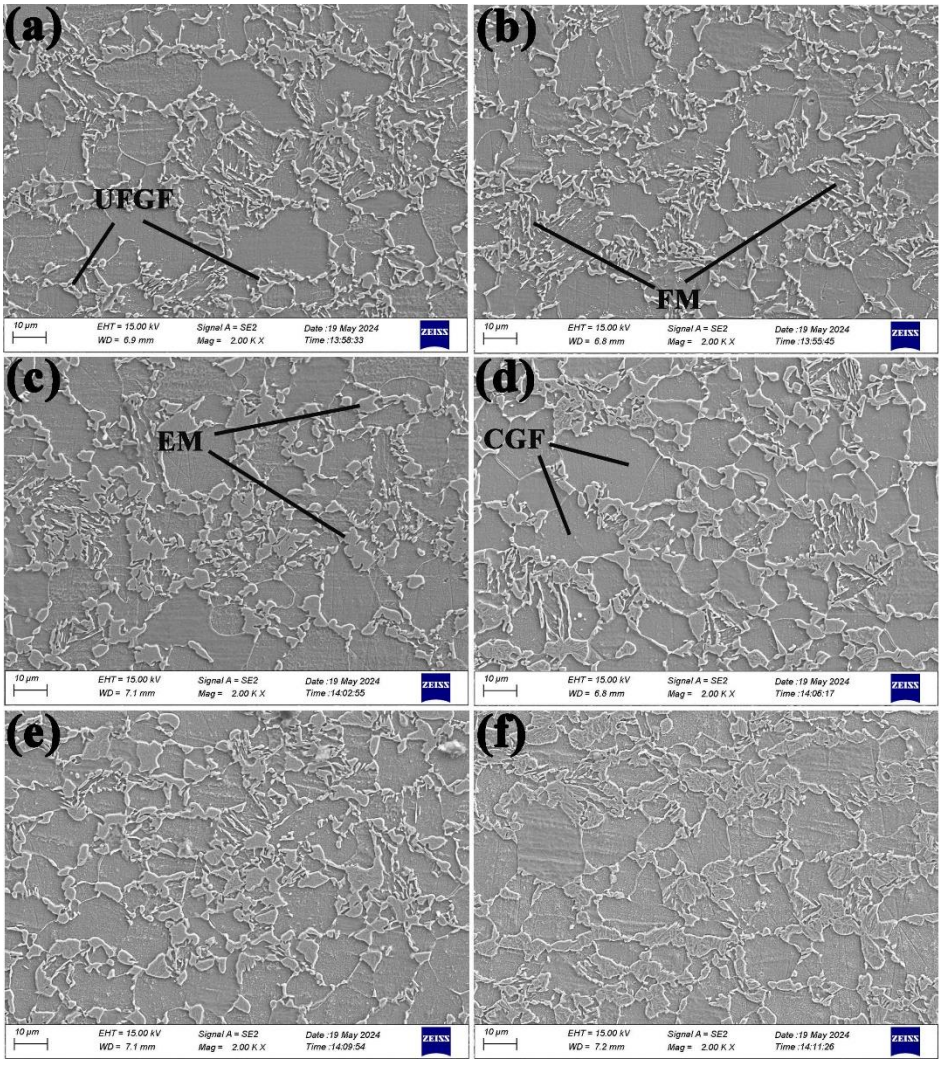

Fig. 3. SEM image of the microstructure of the DP steels obtained from IA heat treatment at: (a) 740 °C for 7 min, (b) 740 °C for 12 min, (c) 770°C for 4 minutes, (d) 770°C for 7 minutes, (e) 770°C for 12 minutes, (f) 800°C for 4 minutes. CGF: coarse-grained ferrite, UFGF: ultrafine-grained ferrite, FM: fibrous martensite, EM: elongated martensite

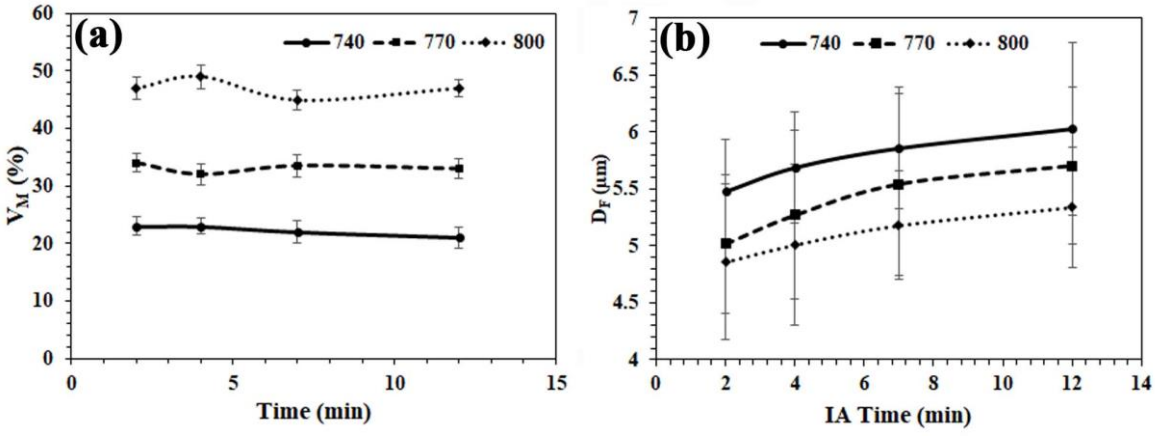

Fig. 4. (a) Volume fraction of martensite (V_M), and (b) average ferrite grain size (D_F) as a function of IA temperature and time.

3.2. Tensile Properties

Fig. 5. shows the engineering stress-strain curves of different samples. The step-quenched sample showed a continuous yielding behavior, characteristic of the DP steels [26, 27]. Similarly, samples annealed at intercritical temperature also showed continuous yielding behavior, with the exception of those annealed at 740°C for 2 and 4 minutes, which displayed a yield-point phenomenon. The austenite to martensite transformation in DP steels is accompanied by a 2-4% volume increase that generates residual stresses in the ferrite and produces geometrically necessary dislocations (GNDs) in the ferrite near the ferrite-martensite interface. The residual stresses are thought to be responsible for lowering the elastic limit, while the GNDs are thought to be the cause of the continuous yielding behavior [28]. The observed yield-point phenomena in samples annealed at 740°C for 2 and 4 minutes indicates that, due to short annealing times, some martensite blocks in the step-quenched sample may have experienced over-tempering instead of forming fresh martensite, similar to heat affected zones of welded DP steels, leading to discontinuous yielding during tensile testing [29]. The appearance of yield point phenomena is attributed to the diffusion of carbon atoms towards free dislocations in ferrite. The tempered martensite islands act as additional sources of carbon. The interaction between carbon atoms and dislocations leads to the discontinuous yielding behavior and enhances the yield stress [30-32].

The changes in tensile properties over different IA times and temperatures are plotted in Fig. 6. It is evident that there is no uniform pattern in the tensile properties at varying temperatures. Generally, samples annealed at 800°C exhibited the highest YS and UTS values, while the highest uniform elongation (UE) and total elongation (TE) values were observed in samples annealed at 740°C. This can be linked to the increase in V_M and the larger size of martensite islands with increasing the IA temperature. Previous researches have clearly shown

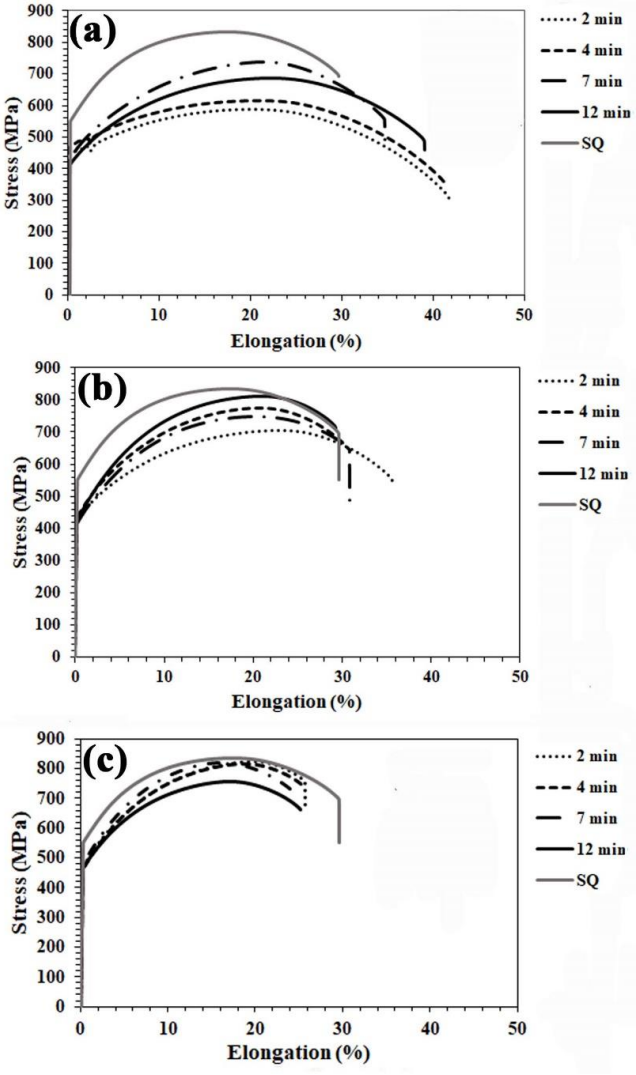

Fig. 5. Engineering stress-strain curves of samples after annealing at different temperatures for various durations: (a) 740°C, (b) 770°C, (c) 800°C.

that the strength of DP steels improves with a larger V_M, while ductility diminishes. Additionally, an increase in the V_M also leads to a decline in ductility [19, 33]. In terms of strength-elongation product, samples annealed at 770°C showed the highest UTS×UE, while annealing at 740°C resulted in the highest UTS×TE. These products are important indicators used in the automotive industry to assess crashworthiness [33]. Therefore, annealing at lower intercritical temperatures, or on the other hand, a lower V_M will result in a better crashworthiness. Overall, the sample annealed at 770°C for 12 minutes displayed the most favorable combination of tensile properties for auto body applications. Despite having lower YS and UTS values compared to the step-quenched sample, the samples annealed at 740°C and 770°C showed improvement in UE and TE. These resulted in a better UTS×UE for most of the samples annealed at 740°C and 770°C compared to the step-quenched sample. However, there was not significant improvement in UTS×TE values and they were even lower in some samples.

3.3. Work Hardening Behavior

The work-hardening behavior of the samples was analyzed using the Modified Crussard–Jaoul (MC-J) analysis [34]:

$$Ln\frac{d\sigma}{d\varepsilon} = (1-m)Ln\sigma - Ln(k'm) \qquad \text{Eq.(3)}$$

Which is based on the Swift equation:

$$\varepsilon = \varepsilon_0 + k'\sigma^m \qquad \text{Eq.(4)}$$

Where σ and ε are true stress and true strain, respectively, m is the inverse of the work-hardening exponent, k′ is the inverse of strength coefficient, and ε_0 is material constant. According to the MC-J analysis, the slope of the Ln ($d\sigma/d\varepsilon$) vs. Ln σ is equal to (1-m). Fig. 7. shows the Ln ($d\sigma/d\varepsilon$) vs. Ln σ plots of samples after IA at different temperatures for various durations. Based on the data shown in the graph, the work-hardening

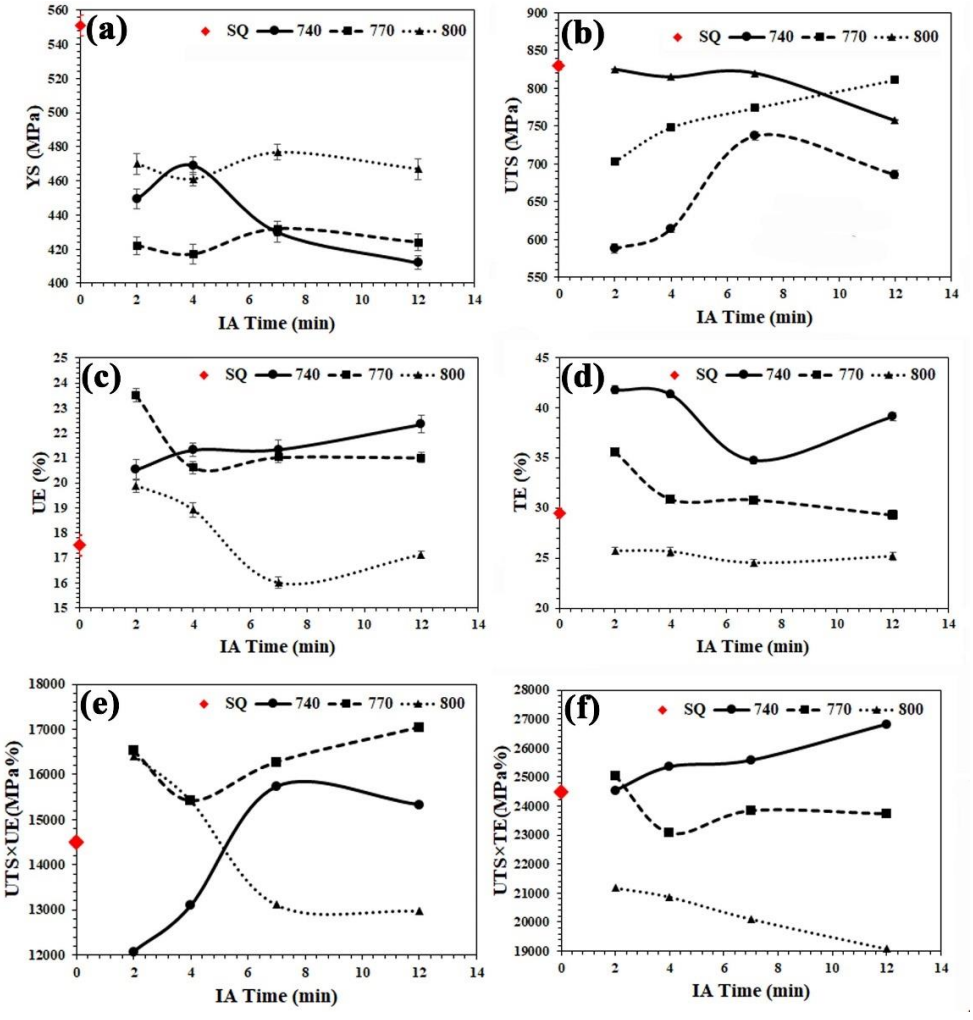

Fig. 6. The variation of tensile properties with IA time at different temperatures, (a) YS, (b) UTS, (c) UE, (d) TE, (e) UTS×UE, (f) UTS×TE.

behavior varied depending on the IA temperature and time. For the samples annealed at 740°C for 2 and 4 minutes (Fig. 7a.), which exhibited discontinuous yielding during the tensile test (Fig. 5a.), a three-stage work-hardening behavior was observed. The first stage (stage I) with the highest slope (i.e. lowest work-hardening ability) is related to the plastic deformation of ferrite. In the second stage (stage II) with the lowest slope (i.e. highest work-hardening ability), the plastic deformation of ferrite is restricted by tempered martensite/martensite islands. The third stage (stage III) with a higher slope compared to the second stage is attributed to plastic deformation in both ferrite and tempered martensite/martensite. Other samples showed a different three-stage work-hardening behavior. The first stage with the lowest slope is related to the plastic deformation of the ferrite matrix. In the second stage with a greater slope, the plastic deformation of ferrite matrix is restrained by the martensite islands. The third stage with the highest slope is corresponded to plastic deformation of both ferrite and martensite [10]. The third stage was absent in samples annealed at 740°C for 7 and 12 min. According to Fig. 4a. samples annealed at 740°C had the smallest V_M among the samples. On the other hand, the carbon concentration of martensite (C_M) in DP steels with a constant chemical composition decreased with increasing the V_M according to the following equation [19]:

$$C_M = \frac{C - C_F(1 - V_M)}{V_M} \qquad \text{Eq.(5)}$$

Where C is the carbon concentration of the steel, and C_F is the supersaturated limit of the carbon in the ferrite phase, which is ~ 0.015wt.%. Therefore, the martensite phase in the samples annealed at 740°C is expected to have the highest C_M. It is commonly known that increasing the carbon content in martensite leads to a decrease in its plasticity. The high carbon content of martensite in the samples annealed at 740°C resulted in a very low ductility of martensite, preventing the martensite phase from co-deforming with the ferrite phase. The difference between the slopes of the work hardening stages of samples annealed at 740°C for 2 and 4 minutes with those for other samples can be attributed to two factors. The first is the absence of GNDs in samples annealed for 2 and 4 minutes at 740°C, and the second is the fact that the martensite in theses samples is over-tempered and is significantly softer than the un-tempered martensite. It is well demonstrated that GNDs are mobile at early stages of plastic deformation and contribute to the initial work hardening behavior, resulting in a different work hardening behavior. Furthermore, the softer tempered martensite can more easily co-deform with the ferrite matrix compared to the un-tempered martensite, resulting in different slopes in stage II and stage III.

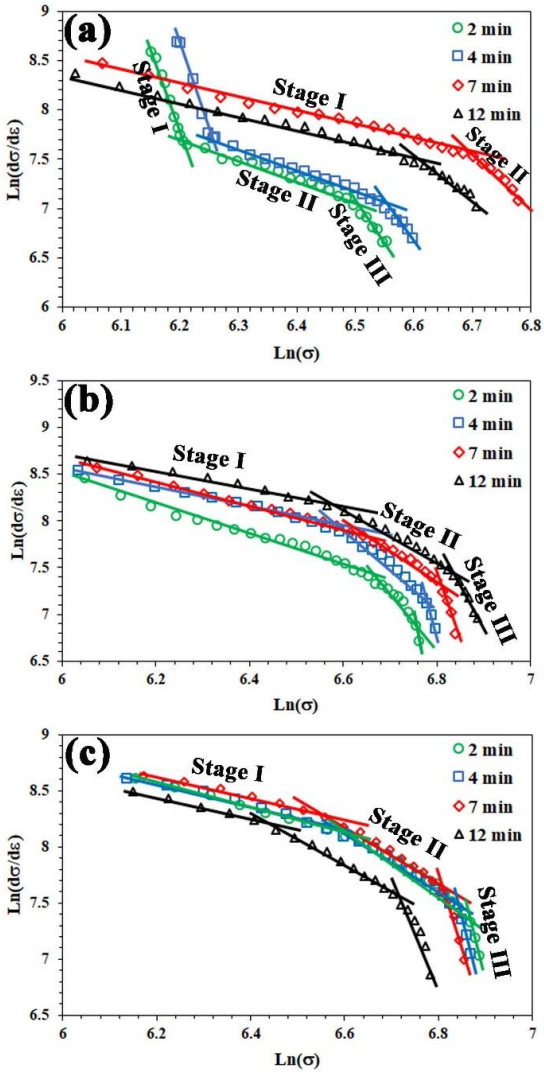

Fig. 7. The Ln (dσ/dε) vs. Ln (σ) plots (MC-J analysis) of the samples annealed for different durations at: (a) 740°C, (b) 770°C, (c) 800°C.

4. Conclusions

In the present work, microstructure and tensile properties of a step-quenched DP steel after IA at 740°C, 770°C and 800°C for 2, 4, 7 and 12 min was investigated. The following are the main conclusions:

- The large martensite blocks in the step-quenched sample were significantly refined after IA. Additionally, the ferrite matrix contained both coarse grains ranging from 10 to 25 μm and ultrafine grains smaller than 2 μm. The martensite islands also had two morphologies: fine and fibrous which mainly observed in samples annealed at 740°C and 770°C, and equiaxed martensite islands which were present in all samples.
- All samples showed continuous yielding behavior except those annealed at 740°C for 2 and 4 min. The

YS and UTS decreased after IA, while UE and TE were improved only after IA at 740°C and 770°C. This resulted in a better UTS×UE for most of the samples annealed at 740°C and 770°C compared to the step-quenched sample, while there was no significant improvement in UTS×TE values. Overall, the sample annealed at 770°C for 12 min showed the best combinations of tensile properties for auto body applications.

- Examination of the work-hardening behavior using the MC-J method indicated a three-stage behavior in all samples. The third stage was not present in the samples annealed at 740°C for 7 and 12 minutes due to the high carbon concentration of martensite.

References

[1] Fonstein N, Dual-phase steels, In: Rana R, Singh SB, editors. Automotive Steels: Design, Metallurgy, Processing and Applications. Woodhead Publishing; 2017: 169-216.

[2] Ogatsu K, Ogawa T, Chen T.T, Sun F, Adachi Y, Dramatic improvement in strength–ductility balance of dual-phase steels by optimizing features of ferrite phase, J Mater Res Technol. 2025; 35: 289-297.

[3] Ashrafi H, Aghili S.E, Study on the micro-texture and anisotropy of a cold-rolled and intercritically annealed DP800 steel, Phys Met Metallogr. 2023; 124: 1426-1432.

[4] Ashrafi H, Shamanian M, Sanayei M, Szpunar J.A, EBSD study of the effect of post-weld intercritical annealing on the microstructure and micro-texture of a friction stir welded DP600 steel, Metallogr Microstruct Anal. 2024; 13: 425–435.

[5] Yang X, Zhao H, Shen G, Peng Y, Wu L, Wu Y, et al. Effect of compressive load on texture evolution and anisotropic behavior of dual-phase steel under biaxial loading in complete σ11-σ22 space, J Mater Res Technol. 2023; 27: 5140–5153.

[6] Dastur P, Slater C, Moore T, Davis C, Martensite size and morphology influence on strain distribution and micro-damage evolution in dual-phase steels; comparing segregation-neutralised and banded grades, Mater Des. 2024; 246: 113340.

[7] Ashrafi H, Mashayekhi F, Microstructure and tensile properties of laser welded joints between DP590 and plain low carbon steels, Int J ISSI. 2023; 20: 53-62.

[8] Wang X, Xu Y, Guo J, Wang Y, Ren J, Misra R.D.K, Tailoring the microstructure by prior treatment to achieve 37.6 GPa·% PSE in a room-temperature quenched and partitioned steel, Mater Charact. 2024; 218: 114497.

[9] Deng Y.G, Yang Y.P, Fine-grained dual-phase steels fabricated via cold-rolling ferrite-martensite structure and subsequent intercritical annealing, J Mater Res Technol. 2023; 27: 3881-3886.

[10] Ghateyi Kalashami A, Kermanpur A, Najafizadeh A, Mazaheri Y, Effect of Nb on microstructures and mechanical properties of an ultrafine-grained dual phase steel, J Mater Eng Perform. 2015; 24: 3008–3017.

[11] Saeidi N, Ashrafizadeh F, Niroumand B, Development of a new ultrafine grained dual phase steel and examination of the effect of grain size on tensile deformation behavior, Mater Sci Eng A. 2014; 599: 145-149.

[12] Nikkhah S, Mirzadeh H, Zamani M, Fine tuning the mechanical properties of dual phase steel via thermomechanical processing of cold rolling and intercritical annealing, Mater Chem Phys. 2019; 230: 1-8.

[13] Mazaheri Y, Kermanpur A, Najafizadeh A, Saeidi N, Effects of initial microstructure and thermomechanical processing parameters on microstructures and mechanical properties of ultrafine grained dual phase steels, Mater Sci Eng A. 2014; 612: 54-62.

[14] Ashrafi H, Shamanian M, Emadi R, Saeidi N, A novel and simple technique for development of dual phase steels with excellent ductility, Mater Sci Eng A. 2017; 680: 197-202.

[15] Ghaemifar S, Mirzadeh H, Enhanced mechanical properties of dual-phase steel by repetitive intercritical annealing, Can Metall Q. 2017; 56: 459-463.

[16] Khebreh-Farshchi Y, Mirzadeh H, Tavakoli M, Zamani M, Microstructure tailoring for property improvements of DP steel via cyclic intercritical annealing, Mater Res Express. 2019; 6: 126513.

[17] Saenarjhan N, Lothongkum G, Opapaiboon J, The effects of double intercritical annealing on microstructure and mechanical properties of 0.107C-2.39Mn-0.453Si dual phase steel, J Met Mater Miner. 2022; 32: 109-117.

[18] Ding C, Liu J, Ning B, Huang M, Wu H, Enhanced strength-plasticity matching of lamellar 1 GPa-grade dual-phase steels via cyclic intercritical quenching, J Mater Res Technol. 2023; 22: 3115-3131.

[19] Ashrafi H, Shamanian M, Emadi R, Saeidi N, Correlation of tensile properties and strain hardening behavior with martensite volume fraction in dual-phase steels, Trans Indian Inst Met. 2017; 70: 1575–1584.

[20] ASTM E112-13. Standard Test Methods for Determining Average Grain Size. ASTM; 2021.

[21] ASTM E562-19. Standard Test Method for Determining Volume Fraction by Systematic Manual Point Count. ASTM; 2019.

[22] Ashrafi H, Shamanian M, Emadi R, Saeidi N, Examination of phase transformation kinetics during step quenching of dual phase steels, Mater Chem Phys. 2017; 187: 203-217.

[23] Ahmad E, Manzoor T, Ziai M.M.A, Hussain N. Effect of martensite morphology on tensile deformation of dual-phase steel, J Mater Eng Perform. 2012; 21: 382–387.

[24] Ashrafi H, Sadeghzade S, Emadi R, Shamanian M, Influence of heat treatment schedule on the tensile properties and wear behavior of dual phase steels, Steel Res Int. 2017; 88: 1600213.

[25] Mazaheri Y, Kermanpour A, Najafizadeh A, Strengthening mechanisms of ultrafine grained dual

phase steels developed by new thermomechanical processing, ISIJ Int. 2015; 55: 218-226.
[26] Maleki M, Mirzadeh H, Zamani M, Effect of intercritical annealing on mechanical properties and work-hardening response of high formability dual phase steel, Steel Res Int. 2018; 89: 1700412.
[27] Kalhor A, Soleimani M, Mirzadeh H, Uthaisangsuk V, A review of recent progress in mechanical and corrosion properties of dual phase steels, Arch Civ Mech Eng. 2020; 20: 85.
[28] Ghassemi-Armaki H, Maaß R, Bhat S.P, Sriram S, Greer J.R, Kumar K.S, Deformation response of ferrite and martensite in a dual-phase steel, Acta Mater. 2014; 62: 197-211.
[29] Mostaan H, Saeedpour P, Ahmadi H, Nouri A, Laser welding of dual-phase steels with different silicon contents: Phase evolutions, microstructural observations, mechanical properties, and fracture behavior, Mater Sci Eng A. 2021; 811: 140974.
[30] Dong D, Liu Y, Yang Y, Li J, Ma M, Jiang T, Microstructure and dynamic tensile behavior of DP600 dual phase steel joint by laser welding, Mater Sci Eng A. 2014; 594: 17-25.
[31] Ramazani A, Bruehl S, Gerber T, Bleck W, Prahl U, Quantification of bake hardening effect in DP600 and TRIP700 steels, Mater Des. 2014; 57: 479-486.
[32] Ramazani A, Bruehl S, Abbasi M, Bleck W, Prahl U, The effect of bake-hardening parameters on the mechanical properties of dual-phase steels, Steel Res Int. 2016; 87: 1559-1565.
[33] Mazaheri Y, Kermanpour A, Najafizadeh A, Microstructures, mechanical properties, and strain hardening behavior of an ultrahigh strength dual phase steel developed by intercritical annealing of cold-rolled ferrite/martensite, Metall Mater Trans A. 2015; 46: 3052-3062.
[34] Mazaheri Y, Jahanara A.H, Sheikhi M, Ghatei-Kalashamib A, High strength-elongation balance in ultrafine grained ferrite-martensite dual phase steels developed by thermomechanical processing, Mater Sci Eng A. 2019; 761: 138021.